Monomeric and Oligomeric Complexes of Ruthenium and Osmium with Tetra-2-pyridyl-1,4-pyrazine (TPPZ)

Claudia R. Arana and Héctor D. Abruña*

Department of Chemistry, Baker Laboratory, Cornell University, Ithaca, New York 14853-1301

Received March 11, 1992

We have prepared a series of monometallic and homo- and heterodimetallic and -trimetallic complexes of Ru and Os with the ligand tetra-2-pyridyl-1,4-pyrazine (tppz) along with mixed-ligand complexes with terpyridine and vinylterpyridine. Their electrochemical and spectroscopic properties were studied and are reported herein. All monometallic complexes were found to be luminescent at both room and liquid-nitrogen temperatures. Electrochemical measurements of dimetallic and trimetallic complexes point to metal–metal interactions as well as to modulations in the π-accepting character of the bridging pyrazine ligand induced by the metal centers.

Introduction

In recent years, the synthesis of oligo- and polymeric transition metal complexes capable of electronic communication between luminescent and redox active sites has been extensively studied.[1] Complexes which incorporate polypyridine-type ligands are particularly attractive because they form very stable complexes with a wide range of transition metals and also stabilize complexes in multiple oxidation states.[2] Their luminescent and redox properties have been extensively studied,[3] and some, which are capable of binding more than one metal, have been found to act as excellent bridges that enhance electronic communication between metal centers.[4] Recently Balzani and co-workers have demonstrated the use of transition metal complexes based on polypyridine type ligands as "building blocks" for the construction of diverse oligomeric complexes.[5]

The ligand tetra-2-pyridyl-1,4-pyrazine (tppz; Figure 1A) was first reported by Goodwin and Lyons[6] and there have been reports on the synthesis and characterization of some transition metal complexes with Fe, Ni, Co, Cu, and Ru.[6,7] In addition, some dimetallic complexes utilizing tppz have also been recently reported.[8,9]

In this paper, we report the synthesis and electrochemical and spectroscopic characterization of monomeric, dimetallic, and a trimetallic complex of ruthenium and osmium with tppz and with terpyridine and vinyl terpyridine. We have studied, in detail, the electrochemical properties of monomers and mixed-ligand complexes as well as dimetallic and trimetallic complexes. These electrochemical measurements point to significant metal–metal interactions as well as to modulations of the π-accepting character of the bridging pyrazine ligand induced by the metal centers.

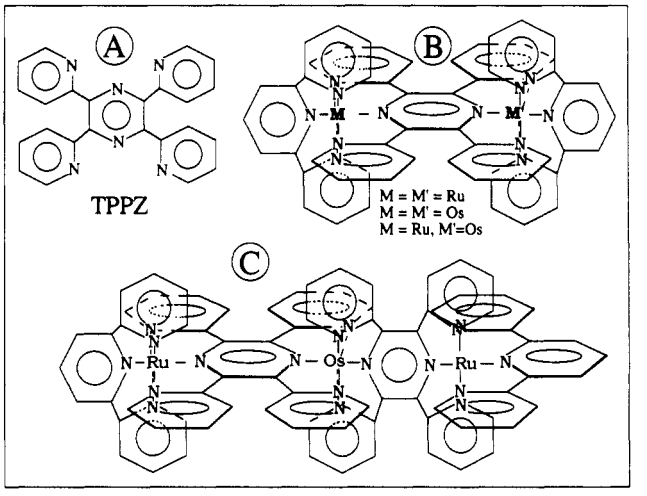

Figure 1. Pictorial depiction for (A) the tppz ligand, (B) the dimetallic complex (tpy)M(tppz)M(tpy)$^{4+}$ and (C) the trimetallic complex (tpy)-Ru(tppz)Os(tppz)Ru(tpy)$^{6+}$.

Experimental Section

Materials and Instrumentation. Electrochemical and spectroscopic measurements were performed in acetonitrile (Burdick and Jackson distilled in glass, dried over 4-Å molecular sieves), water (purified by passage through a Milli-Q purification system), or methylene chloride (Fisher, distilled from CaH_2). The supporting electrolytes were tetrabutylammonium perchlorate (TBAP) (G. F. S. Chemicals), which was recrystallized three times from ethyl acetate and dried under vacuum for 72 h, or sodium perchlorate (Aldrich), which was used as received. The supporting electrolyte concentration was typically 0.10 M. All electrochemical experiments were performed using a platinum-disk working electrode (A = 0.008 cm^2) sealed in glass or a glassy-carbon disk electrode (A = 0.045 cm^2), each of which was polished prior to use with 1-μm diamond paste (Buehler) and rinsed thoroughly with water and acetone. All potentials are referenced to the saturated sodium calomel electrode (SSCE) without regard for the liquid junction potential. A coiled platinum wire was used as a counter electrode and electrochemical cells were of conventional design. Solutions for electrochemistry were typically 0.1–1.0 mM in the redox-active species and were deoxygenated by purging with prepurified nitrogen for at least 10 min. Unless otherwise stated, the sweep rate in cyclic voltammetric experiments was 100 mV/s.

Tetra-2-pyridyl-1,4-pyrazine was prepared according to literature methods,[6] recrystallized three times from pyridine and dried under vacuum for 72 h. 4′-Vinyl-2,2′:6′,2″-terpyridine (v-tpy) was prepared as previously

(1) (a) *Supramolecular Photochemistry*; Balzani, V., Ed.; Reidel: Dordrecht, The Netherlands, 1987. (b) Meyer, T. J. *Acc. Chem. Res.* **1989**, *22*, 163. (c) *Supramolecular Photochemistry*; Balzani, V., Scandola, F., Eds.; Horwood: Chichester, U.K., 1990.
(2) (a) Juris, A.; Balzani, V.; Barigelletti, F.; Campagna, S.; Belser, P.; Von Zelewsky, A. *Coord. Chem. Rev.* **1988**, *84*, 85. (b) Ghosh, B. K.; Chakravorty, A. *Coord. Chem. Rev.* **1985**, *95*, 239. (c) DeArmond, M. K.; Carlin, C. M. *Coord. Chem. Rev.* **1981**, *36*, 325.
(3) (a) Meyer, T. J. *Pure Appl. Chem.* **1986**, *58*, 1193. (b) Kalyanasundaram, K. *Coord. Chem. Rev.* **1982**, *46*, 159.
(4) Steel, P. J. *Coord. Chem. Rev.* **1990**, *106*, 227 and references therein.
(5) (a) Denti, G.; Campagna, S.; Sabatino, L.; Serroni, S.; Ciano, M.; Balzani, V. *Inorg. Chem.* **1990**, *29*, 4750. (b) Denti, G.; Campagna, S.; Sabatino, L.; Serroni, S.; Ciano, M.; Balzani, V. *Inorg. Chim. Acta* **1990**, *29*, 4750. (c) Campagna, S.; Denti, G.; Sabatino, L.; Serroni, S.; Ciano, M.; Balzani, V. *Gazz. Chim. Ital.* **1989**, *176*, 175. (d) Denti, G.; Campagna, S.; De Rosa, G.; Sabatino, L.; Ciano, M.; Balzani, V. *Inorg. Chem.* **1989**, *28*, 2565.
(6) Goodwin, H. A.; Lyons, F. *J. Am. Chem. Soc.* **1959**, *81*, 6415.
(7) Ruminski, R. R.; Letner, C. *Inorg. Chim. Acta* **1989**, *162*, 175.
(8) (a) Petersen, J. D.; Morgan, L. W.; Hsu, I.; Billadeau, M. A.; Ronco, S. E. *Coord. Chem. Rev.* **1991**, *111*, 319. (b) Ruminski, R. R.; Kiplinger, J. L. *Inorg. Chem.* **1990**, *29*, 4581. (c) Du Preez, J. G. H.; Gerber, T. I. A.; Gibson, M. L.; Geyser, R. *J. Coord. Chem.* **1990**, *22*, 249. (d) Ruminski, R. R.; Kiplinger, J. L.; Cockroft, T.; Chase, C. *Inorg. Chem.* **1989**, *29*, 370.
(9) Thummel, R. P.; Chirayil, S. *Inorg. Chim. Acta* **1988**, *154*, 77.

0020-1669/93/1332-0194$04.00/0

described.[10] Terpyridine (tpy), $(NH_4)_2OsCl_6$ (Aldrich Chemical Co.) and $RuCl_3 \cdot 3H_2O$ (Strem Chemical Co.) were used as received. The precursor complexes, $Ru(tpy)Cl_3$ and $Os(tpy)Cl_3$, as well as the reference complexes, $Ru(tpy)_2(PF_6)_2$ and $Os(tpy)_2(PF_6)_2$, were prepared as previously described.[11,12] The synthesis and characterization of the complex $Fe(tppz)_2(PF_6)_2$ was described elsewhere.[13] All other reagents were of at least reagent grade quality and were used without further purification.

Electrochemical experiments were performed using either a Pine Instrument Co. electrochemical analyzer, Model RDE3, or an IBM EC 225 voltammetric analyzer. Data were recorded on a Soltec Model VP-6423S recorder.

Ultraviolet-visible spectra were obtained using a Hewlett-Packard 8451A diode array spectrophotometer in conventional 1-cm quartz cells. Luminescence experiments were performed on a Spex Fluorolog 2 Series spectrofluorimeter.

Mass spectral data was obtained on a Kratos MS-890 spectrometer.

Synthesis of Complexes. $Ru(tppz)_2(PF_6)_2$ and $Ru_2(tppz)_3(PF_6)_4$. To a solution of ruthenium (III) trichloride, (47.4 mg, 177 μmol) in ethanol/water (1:1) (100 mL), was added tppz (283.4 mg, 730 μmol). The solution was purged with nitrogen for 20 min, stirred, and heated at reflux for 48 h until no further color change was observed. The resulting purple solution was allowed to cool and filtered to remove any unreacted tppz. Upon addition of an aqueous saturated solution of ammonium hexafluorophosphate, a purple-black precipitate formed which was collected by filtration. The product was chromatographed on neutral alumina with acetonitrile/toluene (1:1) as eluant. The monomeric product $Ru(tppz)_2(PF_6)_2$ eluted first as an orange band and was followed by the dimetallic product $Ru_2(tppz)_3(PF_6)_4$, which eluted as a purple band. Both materials were recovered by evaporation and dried under vacuum for 24 h. The yields for the mono- and dimetallic complexes were 98.1 mg (46.7%) and 25.0 mg (14.3%), respectively.

$Os(tppz)_2(PF_6)_2$ and $Os_2(tppz)_3(PF_6)_4$. To a solution of ammonium hexachloroosmate (33.9 mg, 77.0 μmol) in ethylene glycol (20 mL) was added tppz (60.3 mg, 155.0 μmol) with stirring. The solution was purged with nitrogen for 15 min, stirred, and heated at reflux for 12 h. The resulting black solution was allowed to cool, filtered to remove any unreacted ligand, and diluted with water (20 mL). A saturated solution of aqueous ammonium hexafluorophosphate was added with stirring until no additional precipitate formed. The black-brown powder was collected by filtration and purified by column chromatography on neutral alumina using acetonitrile/toluene (2:1) as eluant. The first band that eluted yielded the brown product $Os(tppz)_2(PF_6)_2$ whereas a second band yielded the purple dimetallic product $Os_2(tppz)_3(PF_6)_4$. A darker colored material remained at the top of the column and probably consisted of higher oligomers. The yields for the monometallic and the dimetallic complexes were 50.8 mg (52.4%) and 12.0 mg (14.5%), respectively.

$Ru(tpy)(tppz)(PF_6)_2$ and $(Ru(tpy))_2(tppz)(PF_6)_4$. To a solution of $Ru(tpy)Cl_3$ (16.9 mg, 38.3 μmol) in ethanol/water (1:1) was added tppz (15.4 mg, 39.7 μmol). The solution was purged with nitrogen for 15 min and heated at reflux for 12 h. The orange mixed-ligand product $Ru(tpy)(tppz)(PF_6)_2$ was isolated and purified as previously described for $Ru(tppz)_2(PF_6)_2$. $Ru(tpy)(tppz)(PF_6)_2$ eluted first as an orange band and was followed by the dimetallic complex $(Ru(tpy))_2(tppz)(PF_6)_4$ as a purple band. Both products were recovered by evaporation and the yields for the mono- and dimetallic complexes were 16.0 mg (41%) and 2.6 mg (10.1%), respectively.

$Ru(tppz)_2(Ru(tpy))(PF_6)_4$. This complex was prepared by combining $Ru(tppz)_2(PF_6)_2$ (26.6 mg, 22.8 μmol) and $Ru(tpy)Cl_3$ (20.0 mg, 45.0 μmol) in propanol/water (1:1) (10 mL). It was prepared, isolated, and purified using the same procedures described for $(Ru(tpy))_2(tppz)(PF_6)_4$. Yield: 10.2 mg (25%).

$Os(tpy)(tppz)(PF_6)_2$ and $(Os(tpy))_2(tppz)(PF_6)_4$. To a solution of $Os(tpy)Cl_3$ (42.8 mg, 80.5 μmol) in ethylene glycol (25 mL) was added tppz (33.5 mg, 86.3 μmol). The solution was purged with nitrogen for 15 min, heated at reflux for 12 h, cooled, and filtered. Upon addition of water (50 mL) and a concentrated aqueous solution of ammonium hexafluorophosphate, a brown powder precipitated, which was collected by filtration. The product was isolated and purified by chromatography as described for the other monomeric complexes. $Os(tpy)(tppz)(PF_6)_2$ eluted first as a brown band, and the dimetallic complex $(Os(tpy))_2(tppz)(PF_6)_4$ followed as a purple band. The products were recovered by evaporation and dried under vacuum for 24 h. The yields for the monometallic and the dimetallic complexes were 25.8 mg (29%) and 8.1 mg (11.1%), respectively.

$(tpy)M(tppz)M'(tpy)(PF_6)_4$, (M–M' = Ru–Ru, Os–Os, Ru–Os) and $(Ru(v\text{-}tpy))_2(tppz)(PF_6)_4$. Homodimetallic complexes were obtained as byproducts of the reactions to prepare the monometallic mixed-ligand complexes $M(tpy)(tppz)(PF_6)_2$, (M = Ru, Os) as described above. Following the same procedures for the preparation, isolation, and purification of the osmium complexes, we also prepared the dimetallic complex $(Ru(tpy))_2(tppz)(PF_6)_4$ by reacting $Ru(tpy)(tppz)(PF_6)_2$ (10 mg, 9.9 μmol) and $Ru(tpy)Cl_3$ (8.6 mg, 19.9 μmol) in propanol/water (1:1). The dimetallic osmium complex was prepared in the same manner by reacting $Os(tpy)Cl_3$ (13.6 mg, 25.6 μmol) and $Os(tpy)(tppz)(PF_6)_2$ (14.1 mg, 12.8 μmol) in ethylene glycol (10 mL). Both purple dimetallic products were isolated and purified as described for the monometallic complexes. The yield for $(Os(tpy))_2(tppz)(PF_6)_4$ was 2.2 mg (9.4%), and for $Ru(tpy))_2(tppz)(PF_6)_4$, it was 5.1 mg (31%).

The heterodimetallic complex $(tpy)Ru(tppz)Os(tpy)(PF_6)_4$ was also prepared, isolated, and purified by following the same procedure by reacting $Os(tpy)(tppz)(PF_6)_2$ (9.3 mg, 8.4 μmol) and $Ru(tpy)Cl_3$ (7.0 mg, 15.9 μmol) in ethylene glycol (10 mL). Yield: 3.2 mg (22%).

The electropolymerizable dimetallic complex $(Ru(v\text{-}typ))_2(tppz)(PF_6)_4$ was prepared by combining $Ru(v\text{-}tpy)Cl_3$ (where v-tpy = 4′-vinyl-2,2′:6′,2″-terpyridine (18.4 mg, 38.5 μmol); $Ru(v\text{-}tpy)Cl_3$ was prepared in the same manner as $Ru(tpy)Cl_3$) and tppz (7 mg, 18.0 μmol) in ethylene glycol. The complex was isolated and purified using the same procedure described for $Os(tpy)(tppz)(PF_6)_2$. Yield: 10.0 mg (33%). A pictorial depiction for $[(tpy\text{-}M)_2tppz]^{+4}$ complexes is presented in Figure 1B.

$Os(tppz)_2(Ru(tpy))_2(PF_6)_6$. To a solution of $Ru(tpy)Cl_3$ (5.5 mg, 12.5 μmol) in ethylene glycol (2 mL) was added $Os(tppz)_2(PF_6)_2$ (5.1 mg, 4.0 μmol). The solution was purged with nitrogen, stirred, and heated at reflux for 12 h. The purple solution was cooled and filtered. The product was isolated by precipitating with aqueous ammonium hexafluorophosphate. The yield for this product, 6.5 mg (65%), was much greater than that for all other compounds because it was not purified by column chromatography, which in all other cases led to a significant loss of material due to adsorption. The complex was purified by copious washing with water to remove any unreacted $Ru(tpy)Cl_3$ and precipitated from acetone with diethyl ether. A pictorial depiction of the trimer is presented in Figure 1C.

Characterization of Complexes by Fast Atom Bombardment Mass Spectrometry. Elemental analysis alone generally does not provide sufficient information to adequately characterize multimetallic complexes with repeating units. To better characterize these complexes, we utilized fast atom bombardment (FAB) mass spectrometry with 3-nitrobenzyl alcohol as matrix. A compilation of the peaks of highest mass in the spectrum of each complex, and their assignments, is presented in Table I. In general, the FAB mass spectra of all complexes contained numerous informative peaks with isotopic distributions very close to calculated values. In addition, FAB was found to be a relatively soft ionization technique for these complexes since many of the fragment ions observed only involved sequential loss of counterions. In many cases, the inner sphere metal–ligand coordination was left intact, thus making peak identification relatively simple. In all cases, the mass spectral data were consistent with proposed stoichiometries.[14]

Results and Discussion

Electrochemical Measurements. The cyclic voltammetric data for the ruthenium and osmium tppz complexes are presented in Table II. In general, the monomeric complexes exhibited one metal-based oxidation at positive potentials corresponding to the M(II/III) couple. In the negative potential region, the redox processes observed were sequential ligand-based reductions. Generally tppz-based reductions were observed at less negative potentials than the corresponding processes for tpy.

(10) Potts, K. T.; Usifer, D. A.; Guadalupe, A.; Abruña, H. D. *J. Am. Chem. Soc.* **1987**, *109*, 3963.

(11) (a) Adcock, P. A.; Keene, F. R.; Smythe, R. S.; Snow, M. R. *Inorg. Chem.* **1984**, *23*, 2236. (b) Kober, E. M.; Caspar, J. V.; Sullivan, B. P.; Meyer, T. J. *Inorg. Chem.* **1988**, *27*, 4587.

(12) (a) Young, R. C.; Nagle, J. K.; Meyer, T. J.; Whitten, D. G. *J. Am. Chem. Soc.* **1978**, *100*, 4773. (b) Stone, M. L.; Crosby, G. A. *Chem. Phys. Lett.* **1981**, *79*, 169. (c) Kober, E. M.; Marshall, J. L.; Dressick, W. J.; Sullivan, B. P.; Caspar, J. V.; Meyer, T. J. *Inorg. Chem.* **1985**, *24*, 2755.

(13) Arana, C. R.; Yan, S.; Keshavarz-K, M.; Potts, K. T.; Abruña, H. D. *Inorg. Chem.* **1992**, *31*, 3680.

(14) A complete listing of mass spectral data is available as supplementary material.

Table I. Mass Spectral Data for tppz Complexes of Ruthenium and Osmium

complex	m/z	rel abundance	assignment
$Ru(tppz)_2(PF_6)_2$	1021.1	14.7	$Ru(tppz)_2(PF_6)^+$
	878.2	100	$Ru(tppz)_2^+$
	438.7	48.4	$Ru(tppz)_2^{2+}$
$Os(tppz)_2(PF_6)_2$	1113.1	50	$Os(tppz)_2(PF_6)^+$
	968.2	100	$Os(tppz)_2^+$
	484.1	55	$Os(tppz)_2^{2+}$
$Ru(tpy)(tppz)(PF_6)_2$	1018.3	2	$Ru(tpy)(tppz)(PF_6)_2^+$
	869.0	80	$Ru(tpy)(tppz)(PF_6)^+$
	742.2	40	$Ru(tpy)(tppz)F^+$
	723.2	100	$Ru(tpy)(tppz)^+$
$Os(tpy)(tppz)(PF_6)_2$	958.2	58	$Os(tpy)(tppz)(PF_6)^+$
	828.2	23	$Os(tpy)(tppz)F^+$
	813.3	100	$Os(tpy)(tppz)^+$
	723.2	11	$Os(tppz)(PF_6)^+$
	406.5	65	$Os(tpy)(tppz)^{2+}$
$Os_2(tppz)_3(PF_6)_4$	1835.4	4	$Os_2(tppz)_3(PF_6)_2^+$
	1690.5	25	$Os_2(tppz)_3(PF_6)^+$
	1545.5	27	$Os_2(tppz)_3^+$
	1113.5	21	$Os(tppz)_2(PF_6)^+$
	968.5	55	$Os(tppz)_2^+$
	720.9	100	$Os(tppz)(PF_6)^+$
$Ru_2(tppz)_3(PF_6)_4$	1802.2	5.2	$Ru_2(tppz)_3(PF_6)_3^+$
	1657.5	15.6	$Ru_2(tppz)_3(PF_6)_2^+$
	1512.6	8.6	$Ru_2(tppz)_3(PF_6)^+$
	877.5	100.0	$Ru(tppz)_2^+$
$(Ru(tpy))_2(tppz)(PF_6)_4$	1493	17	$(tpy)Ru(tppz)Ru(tpy)(PF_6)_3^+$
	1348	83	$(tpy)Ru(tppz)Ru(tpy)(PF_6)_2^+$
	1203	76	$(tpy)Ru(tppz)Ru(tpy)(PF_6)^+$
	1055	40	$(tpy)Ru(tppz)Ru(tpy)^+$
	722	100	$(tpy)Ru(tppz)^+$
$(Ru(v\text{-}tpy))_2(tppz)(PF_6)_4$	1547	3.3	$(Ru(v\text{-}tpy))_2(tppz)(PF_6)_3^+$
	1402	15.7	$(Ru(v\text{-}tpy))_2(tppz)(PF_6)_2^+$
	1258	9.5	$(Ru(v\text{-}tpy))_2(tppz)(PF_6)^+$
	750	86	$Ru(v\text{-}tpy)(tppz)^+$
$(Os(tpy))_2(tppz)(PF_6)_4$	1527	28	$(tpy)Os(tppz)Os(tpy)(PF_6)_2^+$
	1383	66	$(tpy)Os(tppz)Os(tpy)(PF_6)^+$
	1235	100	$(tpy)Os(tppz)Os(tpy)^+$
	813	23	$Os(tpy)(tppz)^+$
$Ru(tppz)_2Ru(tpy)(PF_6)_4$	1234	23.2	$Ru(tppz)_2Ru(tpy)H_2F^+$
	765	47.9	$Ru(tppz)Ru(PF_6)^+$
	721	30.1	$Ru(tpy)(tppz)^+$
	594	100	$Ru(tppz)Ru^+$
$Os(tppz)_2(Ru(tpy))_2(PF_6)_6$	1449	16	$Os(tppz)_2Ru(tpy)(PF_6)^+$
	1302	29	$Os(tppz)_2Ru(tpy)^+$
	1216	30	$Os(tppz)_2Ru(PF_6)^+$
	1172	19	$Os(tppz)_2Ru_2^+$
	723	100	$Ru(tpy)(tppz)^+$

Table II. Formal Potentials vs SSCE for Os and Ru Complexes of tppz and Related Complexes at a Platinum Electrode in a 0.1 M Acetonitrile Solution of TBAP (Except Where Indicated, the Processes were One-Electron Transfers)

complex	$E°$ (V) [ΔE_p (mV)]
	Monometallic Complexes
$Ru(tpy)_2(PF_6)_2$[a]	+1.29 [70], −1.25 [50], −1.51 [50]
$Os(tpy)_2(PF_6)_2$[b]	+0.93 [70], −1.20 [60], −1.49 [70]
$Ru(tppz)_2(PF_6)_2$[c]	+1.51 [60], −0.88 [60], −1.10 [60], −1.53 [50], −1.67 [50]
$Os(tppz)_2(PF_6)_2$	+1.23 [70], −0.83 [60], −1.11 [60], −1.48 [60], −1.64 [60]
$Ru(tpy)(tppz)(PF_6)_2$[c]	+1.50 [140], −0.95 [60], −1.40 [70], −1.60 [70]
$Os(tpy)(tppz)(PF_6)_2$	+1.08 [60], −0.97 [60], −1.39 [90], −1.74 [80]
	Dimeric and Trimeric Complexes
$Ru_2(tppz)_3(PF_6)_4$	+1.53 [60], +0.99 [80], −0.29 [60], −0.77 [60], −1.15 ($2e^-$) [180]
$Os_2(tppz)_3(PF_6)_4$	+1.58 [60], +1.18 [50], −0.29 [60], −0.73 [70], −1.12 ($2e^-$) [200]
$(Os(tpy))_2(tppz)(PF_6)_4$	+1.44 [60], +0.97 [60], −0.39 [70], −0.82 [70], −1.35 [irrev], −1.45 [irrev]
$(Ru(tpy))_2(tppz)(PF_6)_4$[c]	+1.71 [60], +1.40 [60], −0.39 [50], −0.86 [50], −1.43 ($2e^-$) [170], −1.86 ($2e^-$) [80]
$(Ru(v\text{-}tpy))_2(tppz)(PF_6)_4$	+1.72 [100], +1.36 [80], −0.41 [50], −0.90 [50], −1.50 ($2e^-$) [100]
$(tpy)Ru(tppz)Os(tpy)(PF_6)_4$	+1.38 [70], +1.11 [70], −0.41 [90], −0.85 [60], −1.55 ($2e^-$) [110]
$Ru(tppz)_2Ru(tpy)(PF_6)_4$	+1.68 [80], +1.38 [60], −0.39 [70], −0.85 [60], −1.43 ($2e^-$) [60]
$(Ru(tpy))_2Os(tppz)_2(PF_6)_6$	+1.72 [60], +1.59 [60], +1.23 [60], −0.30 [60], −0.42 [60], −0.82 [60], −0.97 [60], −1.46 [irrev]

[a] Reference 12a,b. [b] Reference 12c. [c] Reference 9.

Given their similarity in electrochemical behavior, complexes of osmium and ruthenium containing the same ligands will be discussed together.

Monomeric Complexes. $M(tppz)_2(PF_6)_2$ (M = Ru, Os). The cyclic voltammogram of $Ru(tppz)_2(PF_6)_2$ in acetonitrile solution exhibits a reversible, one-electron oxidation at +1.51 V corresponding to a Ru(II/III) couple. As anticipated, this potential is significantly more positive (by about 220 mV) than the corresponding process in $Ru(tpy)_2(PF_6)_2$[12a,b] due to the increased π acidity of tppz relative to tpy. The free tppz ligand exhibits one reduction in acetonitrile solution at −1.65 V and has been shown to exhibit other redox processes.[15] As would be anticipated,

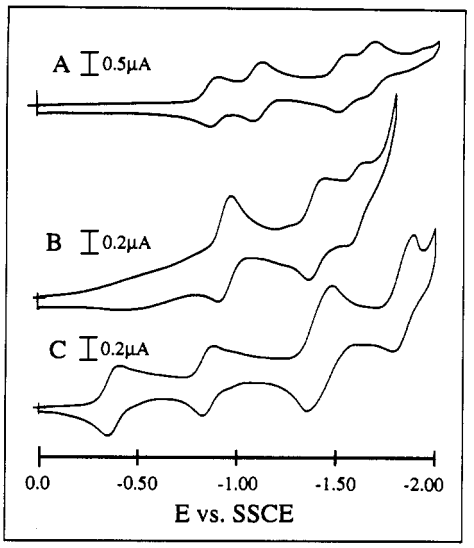

Figure 2. Cyclic voltammograms for the mononuclear complexes (A) $Ru(tppz)_2^{2+}$ and (B) $Ru(tpy)(tppz)^{2+}$ and (C) the dimeric complex $(tpy)Ru(tppz)Ru(tpy)^{4+}$ at a Pt-disk electrode in 0.1 M TBAP/acetonitrile.

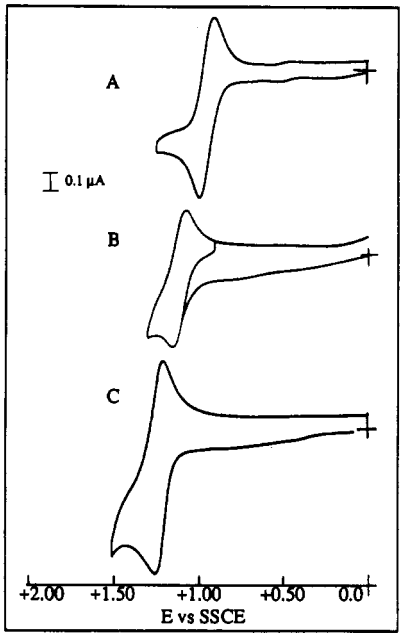

Figure 3. Cyclic voltammograms showing the Os(II/III) oxidation in (A) $Os(tpy)_2^{2+}$, (B) $Os(tpy)(tppz)^{2+}$, and (C) $Os(tppz)_2^{2+}$, at a Pt-disk electrode in 0.1 M TBAP/acetonitrile.

upon coordination to ruthenium, the tppz reductions are shifted to less negative potentials so that one-electron reversible redox processes are observed at potentials of –0.88, –1.10, –1.53, and –1.67 V (Figure 2A) We ascribe the reductions at –0.88 and –1.10 V as due to the first reduction of each tppz ligand, whereas those at –1.53 and –1.67 V correspond to the second reduction.

The analogous osmium complex, $Os(tppz)_2(PF_6)_2$ also has one reversible, one-electron oxidation at +1.23 V corresponding to the Os(II/III) couple (Figure 3C). This oxidation is also significantly more positive (by 300 mV) than the corresponding oxidation in $Os(tpy)_2(PF_6)_2$[12c] (Figure 3A). Furthermore, the difference in potentials between this and the analogous Ru complex is typical of these metals with similar coordination. $Os(tppz)_2(PF_6)_2$ also exhibits four consecutive one-electron ligand based reductions at –0.83, –1.11, –1.48, and –1.64 V (Figure 4C). As mentioned above for the ruthenium complex, the first two processes are ascribed to the first reduction of each tppz ligand, and the

(15) Bock, H.; Jaculi, D. *Z. Naturforsch, B: Anorg. Chem., Org. Chem.* **1991**, *46*, 1091.

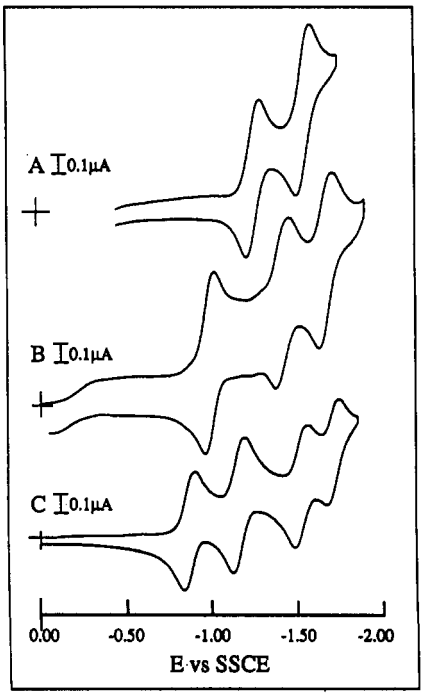

Figure 4. Cyclic voltammograms of (A) $Os(tpy)_2^{2+}$, (B) $Os(tpy)(tppz)^{2+}$, and (C) $Os(tppz)_2^{2+}$, at a Pt-disk electrode in 0.1 M TBAP/acetonitrile.

second two waves correspond to their second reduction. The fact that these potentials are essentially insensitive to the nature of the metal imply that they are largely ligand localized.

$M(tpy)(tppz)(PF_6)_2$ (M = Ru, Os). As mentioned above, monometallic complexes ML_2 (where M = Ru, Os and L = tpy, tppz), exhibit M(II/III) oxidations in the order $M(tpy)_2 < M(tppz)_2$. Therefore, we would anticipate that mixed-ligand complexes ($M(LL')^{+2}$, where L = tpy and L' = tppz) would exhibit M(II/III) oxidations at potentials between those observed for ML_2 complexes. In addition, we would also anticipate ligand based reductions to occur in the order tpy < tppz. This behavior is indeed observed in the tpy/tppz mixed-ligand complexes of osmium and ruthenium. The Ru(II/III) oxidation in the mixed-ligand complex $Ru(tpy)(tppz)(PF_6)_2$ is observed as a one-electron process at +1.50 V. The oxidation potential is considerably more positive than that observed for the Ru(II/III) couple in $Ru(tpy)_2(PF_6)_2$ (+1.29 V) and slightly more negative than the corresponding process for $Ru(tppz)_2(PF_6)_2$ (+1.51 V). The potential that we observe is dramatically different from a value previously reported (+0.97 V) for ostensibly the same complex.[9] However, we believe that this is likely due to either protonation of the uncoordinated pyridine groups in the tppz ligand, which would significantly shift the metal oxidation potential or to an impurity. In a solution containing acetonitrile and 20% HPF_6, the ruthenium oxidation potential was observed at +1.12 V.

Figure 3 shows the cyclic voltammograms for (A) $Os(tpy)_2(PF_6)_2$, for (C) $Os(tppz)_2(PF_6)_2$, and for the mixed-ligand complex, (B) $Os(tpy)(tppz)(PF_6)_2$. The Os(II/III) oxidation in the mixed-ligand complex is observed at +1.08 V, which, as for the analogous ruthenium complex, is at a potential that falls between those of the ML_2 complexes.

Both mixed-ligand complexes of ruthenium and osmium show three reversible, one-electron ligand-based reductions at negative potentials. We assign the one-electron reductions at –0.95 and –1.60 V in the ruthenium complex (Figure 2B) and at –0.97 and –1.74 V in the osmium complex (Figure 3B) to the sequential one-electron reductions of the tppz ligand. The reductions at –1.40 and –1.39 V in the ruthenium and the osmium complexes, respectively, are ascribed to the one-electron reduction of the terpyridine ligand. These assignments are based on the fact that the same potential difference (650 mV) is observed between the

first and second reductions of the tppz ligand in the mixed-ligand complex as in the bis-tppz complex. In addition, the potentials for these reductions in the mixed-ligand complex are quite close (difference of 110 mV) to those observed in the bis-tppz complex. Finally, a 150 mV shift in the of terpyridine-based reduction from the values for the bis-tpy to the mixed-ligand complex is consistent with the potential shifts for the reductions of the tppz ligands between the bis-tppz and the mixed-ligand complexes.

Dimetallic Complexes. In the absence of any metal–metal interaction, one would anticipate that symmetric dimetallic complexes would exhibit metal-based oxidations at the same potential for both metal centers. If there is metal–metal communication through the bridging ligand, such symmetric dimetallic complexes would be expected to exhibit two oxidations since the oxidation of one metal center is influenced by the oxidation of the other. The difference in these potentials can depend on a number of aspects including metal–metal communication across the bridging ligand. In addition, modulation of the binding properties of the bridging ligand by the metal centers can also affect the values of the potentials. In the present case, variations in the π-accepting ability of the bridging pyrazine group would be of particular importance. For the complexes of ruthenium and osmium presented in this study, these oxidation potentials would formally correspond to the following processes:

$$M^{II}\text{–tppz–}M^{II} \overset{E^{\circ\prime}(1)}{\rightleftarrows} M^{II}\text{–tppz–}M^{III} \overset{E^{\circ\prime}(2)}{\rightleftarrows} M^{III}\text{–tppz–}M^{III}$$

The degree of metal–metal interaction in dimetallic complexes has been examined extensively using electrochemical data.[16] Changes in the first oxidation potential between mono- and dimetallic complexes can be indicative of the effect that the second metal unit has on the first. The difference in potential for the first and second oxidations in dimetallic complexes would reflect the stabilization or destabilization of the metal π orbitals (t_{2g}) by coordination of a second metal unit. Such a change could be dictated by variations in the π-accepting ability of the bridge. Finally, the difference in ligand-based reduction potentials between mono- and dimetallic complexes would reflect the stabilization of the π^* orbitals of the tppz ligands upon coordination of a second metal center.

$M_2(tppz)_3(PF_6)_4$ (M = Ru, Os). Based on the above arguments, metal-metal coupling through the tppz ligand appears to be significant. Two Ru(II/III) oxidations are observed at +0.99 and +1.53 V in the dimetallic ruthenium complex $Ru_2(tppz)_3(PF_6)_4$, whereas for the analogous osmium dimer the Os(II/III) redox couples are observed at +1.18 and +1.58 V. The large $\Delta E^{\circ\prime}$ (540 and 400 mV for the ruthenium and osmium dimers, respectively) values observed for these complexes would suggest a high degree of metal–metal interaction through the bridging tppz ligand. In addition, the difference between the first oxidation potentials in the mono- and dimetallic complexes is quite significant in the case of ruthenium (520 mV) albeit smaller for the osmium complex (210 mV).

However, it needs to be pointed out that in addition to metal–metal interactions such differences and/or variations in the redox potentials can arise as a result of modulations in the π accepting properties of the bridigine pyrazine ligands as a result of binding by the second metal center. The importance of this effect has been previously pointed out by Taube et al.[17] in a series of ligand-bridged pentaamine ruthenium and rhodium complexes.

It is also of interest to compare the difference in formal potentials ($\Delta E^{\circ\prime}$) for the ruthenium and osmium complexes in terms of possible effects on the bridging pyrazine's π^* orbitals. Since osmium is a third-row metal, the radial extension of its d orbitals is larger than that of ruthenium. Thus, one would have anticipated that if modulation of the π^* orbitals of the pyrazine were largely responsible for the difference in formal potentials within a dimer, the osmium complex would exhibit a larger difference. However, this is not the case, and this indicates that other effects are playing an important role.

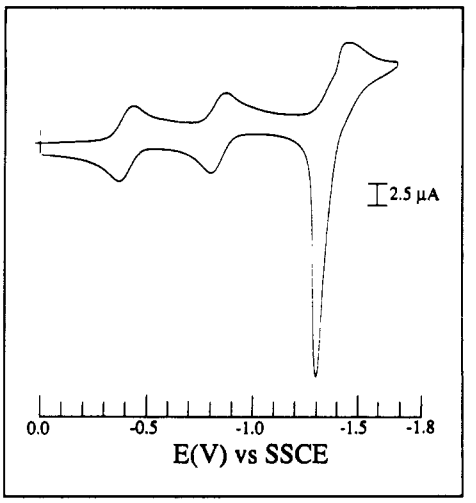

Figure 5. Cyclic voltammogram of the dimeric complex (tpy)Os(tppz)-Os(tpy)$^{+4}$ at a Pt-disk electrode in 0.1 M TBAP/acetonitrile.

These dimetallic complexes exhibit a series of four ligand-based reductions. The bridging tppz ligand is reduced first at a much more positive potential than in the monometallic complex since coordination to two positively charged metal centers significantly withdraws electron density. In addition, the difference in the first ligand-based reduction potential between the mono- and dimetallic complexes reflects the stabilization of the bridging ligand's π^* orbitals by coordination to a second metal center. The ruthenium dimetallic complex has two ligand-based reductions at –0.29 and –0.77 V corresponding to the sequential reduction by one electron of the bridging tppz ligand. The first reduction is shifted by 0.59 V from its value in the monometallic complex $Ru(tppz)_2(PF_6)_2$, indicating a great deal of stabilization of the bridging tppz's π^* orbitals.

$Ru_2(tppz)_3(PF_6)_4$ exhibits an additional two-electron reduction at –1.05 V corresponding to the reduction of the two peripheral tppz ligands. This reduction is then followed by adsorption of the complex on the electrode surface. This is not unusual as the complex is uncharged at this potential and is thus prone to adsorption or precipitation. As the potential is scanned in the negative direction from 0.0 to –0.90 V and reversed, the bridging tppz reductions at –0.29 and –0.77 V appear reversible and their peak current ratios are equal to 1. If the potential is scanned beyond –1.05 V, thus imparting an overall neutral charge on the molecule (vide supra), upon scan reversal there is a large desorption spike at –0.97 V and a smaller one at –0.74 V. If the potential is scanned more negatively, an additional adsorption spike is observed at –1.70 V. Upon scan reversal, two very large desorption spikes are observed at the potentials mentioned above. This behavior is quite similar to that observed for most of the other dimetallic species such as $(Os(tpy))_2(tppz)(PF_6)_4$ (Figure 5).

The ligand-based reductions in the dimetallic osmium complex, $Os_2(tppz)_3(PF_6)_4$, are similar to the analogous ruthenium complex and are observed as one-electron, reversible processes at –0.29 and –0.73 V and as a two-electron process at –1.12 V. Following the same arguments given above for the ruthenium complex, one can assign the first two reductions to the bridging tppz. As before, these processes are also significantly shifted positively with respect to the monometallic complex (by 0.54 V), indicating a significant degree of stabilization of the bridging tppz π^* orbitals. The two-

(16) (a) Scandola, F.; Indelli, M. T.; Chiorboli, C.; Bignozzi, C. A. *Top. Curr. Chem.* **1990**, *158*, 73. (b) Brewer, K. J.; Murphy, Jr., W. R.; Petersen, J. D. *Inorg. Chem.* **1987**, *26*, 3376. (c) Ruminski, R. R.; Cockroft, T.; Shoup, M. *Inorg. Chem.* **1988**, *27*, 4026. (d) Braunstein, C. H.; Baker, A. D.; Strekas, T. C.; Gafney, H. D. *Inorg. Chem.* **1984**, *23*, 857. (e) Creutz, C.; Taube, H. *J. Am. Chem. Soc.* **1973**, *95*, 1086. (f) Creutz, C.; Taube, H. *J. Am. Chem. Soc.* **1969**, *91*, 3988.

(17) (a) Sutton, J. E.; Sutton, P. M.; Taube, H. *Inorg. Chem.* **1979**, *18*, 1017. (b) Sutton, J. E.; Taube, H. *Inorg. Chem.* **1981**, *20*, 3125.

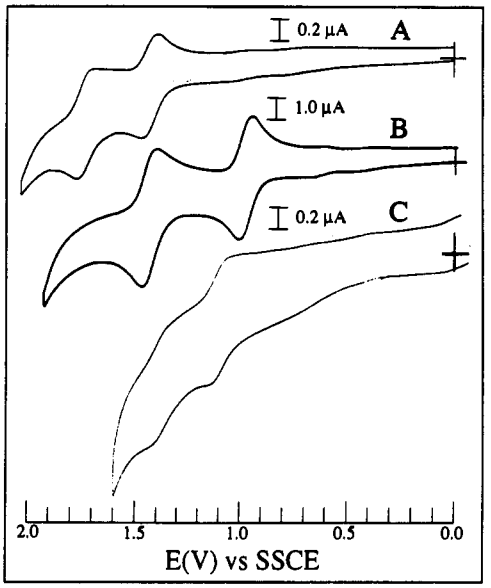

Figure 6. Cyclic voltammograms for the dimetallic complexes (A) (tpy)-Ru(tppz)Ru(tpy)$^{4+}$, (B) (tpy)Os(tppz)Os(tpy)$^{4+}$, and (C) (tpy)Ru(tppz)-Os(tpy)$^{4+}$, at a Pt-disk electrode in 0.1 M TBAP/acetonitrile.

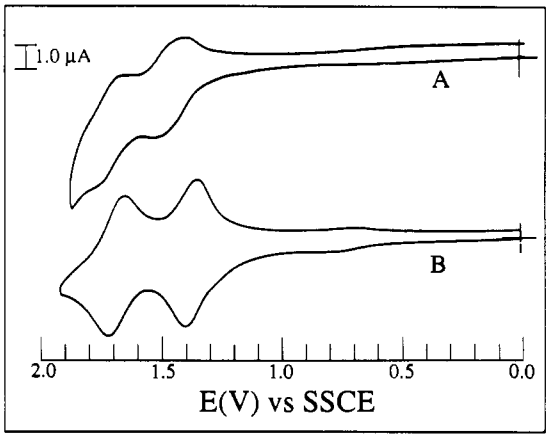

Figure 7. Cyclic voltammograms of (v-tpy)Ru(tppz)Ru(v-tpy)$^{4+}$ at a Pt-disk electrode (A) in solution and (B) electropolymerized on the surface in 0.1 M TBAP/acetonitrile.

electron reduction at −1.12 V corresponds to the simultaneous reduction of the peripheral tppz ligands and also leads to precipitation of the complex on the surface of the electrode. When the potential is scanned beyond −1.20 V, upon reversal there is a large desorption spike at −0.92 V and a smaller one at −0.70 V. If the potential is held beyond −1.20 V for a long period of time the size of the spike increases indicative of precipitation.

(Ru(tpy))$_2$(tppz)(PF$_6$)$_4$ and (Ru(v-tpy))$_2$(tppz)(PF$_6$)$_4$. Thummel and Chirayil previously reported formal oxidation potentials for (Ru(tpy))$_2$(tppz)(PF$_6$)$_4$ at +1.05 and +1.43 V.[9] We had initially observed oxidations at those potentials, as well as an additional wave with a formal potential of +1.71 V. After further purification of the complex by column chromatography, the peak at +1.05 V disappeared. Given our observations and the relative size of the waves in the voltammogram presented by Thummel and Chirayil, we have concluded that the wave at +1.05 V is likely due to an impurity from the mixed-ligand monometallic complex they used as a precursor for the preparation of the dimetallic complex. As with the other dimetallic complexes previously described, (Ru(tpy))$_2$(tppz)(PF$_6$)$_4$ exhibits two oxidations, in this case at +1.40 and +1.71 V (Figure 6A). The significant difference in formal potentials ($\Delta E^{\circ\prime}$ of 310 mV) again points to significant interactions. There is also a significant difference in formal potentials between the first oxidation in the dimetallic complex (+1.40 V) and the oxidation of the mixed-

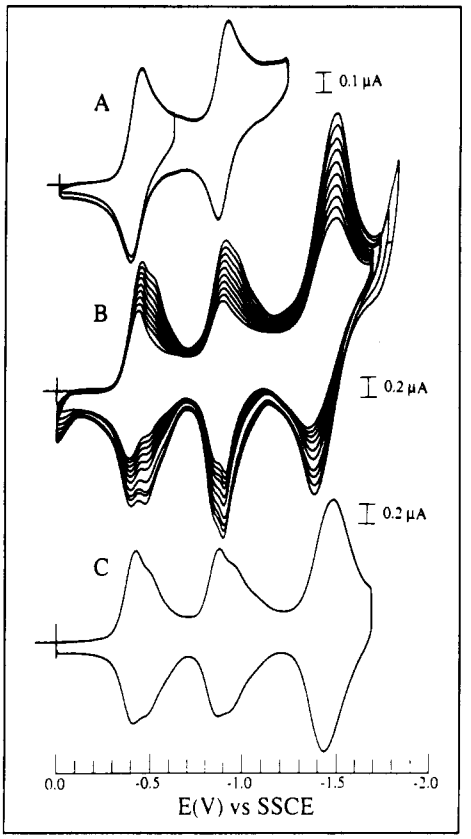

Figure 8. CVs at a Pt-disk electrode in contact with a solution of (v-tpy)Ru(tppz)Ru(v-tpy)$^{4+}$ scanned (A) between 0.0 and −0.6 V and 0.0 and −1.2 V and (B) between 0.0 and −1.7 V (note change in current scale) and (C) at a Pt-disk electrode modified with electropolymerized film of the complex. All CV's were obtained on compounds in 0.1 M TBAP/acetonitrile.

ligand complex Ru(tpy)(tppz)(PF$_6$)$_2$ (+1.50 V), which is also indicative of a high degree of interaction. (Ru(tpy))$_2$(tppz)-(PF$_6$)$_4$ exhibits two reversible one-electron ligand based reductions at −0.39 and −0.86 V, and two two-electron reductions at −1.43 and −1.86 V (Figure 2C). On the basis of the analogous monometallic complexes and the shifts observed when tppz acts as a bridging ligand, we assign the one-electron reductions at −0.39 and −0.86 V to the sequential one-electron reductions of the bridging tppz ligand. The two-electron reduction at −1.43 V corresponds to the simultaneous reduction of the peripheral terpyridine ligands whereas the two-electron reduction at −1.86 V probably corresponds to the additional reductions of the bridging tppz ligands. Unlike the other dimetallic complexes we studied, this compound did not precipitate after reduction at −1.45 V even though it is ostensibly present as a neutral species.

These assignments are further corroborated by the voltammetric response of (Ru(v-tpy))$_2$(tppz)(PF$_6$)$_4$ where the peripheral terpyridines contain an electropolymerizable vinyl group. In solution, (Ru(v-tpy))$_2$(tppz)(PF$_6$)$_4$ exhibits behavior very similar to that of (Ru(tpy))$_2$(tppz)(PF$_6$)$_4$. At positive potentials between 0.0 and +2.0 V, the oxidation of the Ru metal centers are observed at +1.36 and +1.72 V (Figure 6A) whereas in the negative region, the complex exhibits two one-electron processes at −0.41 and −0.90 V and a two-electron wave at −1.50 V. Figure 8A shows the voltammetric response of a freshly polished platinum electrode in contact with a solution of (Ru(v-tpy))$_2$(tppz)(PF$_6$)$_4$ in acetonitrile as the potential is scanned three times between 0.0 and −0.60 V and three times between 0.0 and −1.20 V. As can be observed from the figure, when the electrode is scanned in these potential regions, there is no increase of the current upon scanning, thus demonstrating that no electropolymerization of the complex is taking place. Furthermore, even when the electrode was scanned between 0.0 and −1.20 V for 5 min, rinsed with acetone, and

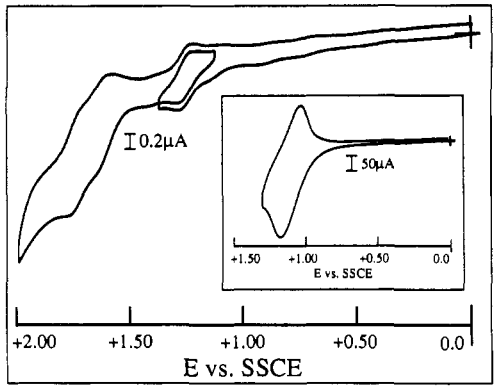

Figure 9. Cyclic voltammogram at a glassy-carbon-disk electrode for the trimetallic complex (tpy)Ru(tppz)Os(tppz)Ru(tpy)$^{6+}$ in 0.1 M TBAP/acetonitrile scanned between 0.0 and +2.0 V. The inset shows the cyclic voltammogram of same complex adsorbed on a glassy-carbon-disk electrode in aqueous 0.1 M $NaClO_4$.

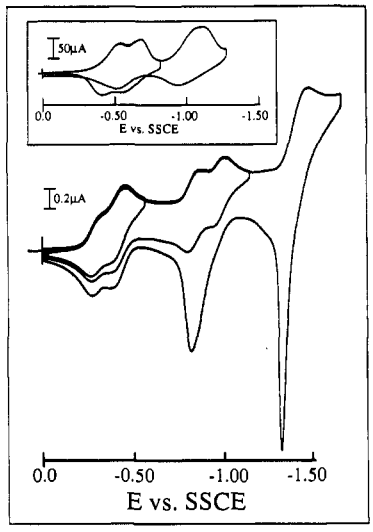

Figure 10. CV at a glassy-carbon electrode for the trimetallic complex (tpy)Ru(tppz)Os(tppz) Ru(tpy)$^{6+}$ in 0.1 M TBAP/acetonitrile scanned between 0.0 and −1.6 V. The inset shows the cyclic voltammogram of same complex adsorbed on a glassy-carbon-disk electrode in aqueous 0.1 M $NaClO_4$.

placed in a solution containing only supporting electrolyte, only background current was observed. These observations are in agreement with the assignment of these waves as reductions of the bridging tppz ligand. Since the vinyl groups are on the terpyridine groups, reductions of the bridging tppz ligand are not expected to effect any polymerization. Figure 8B shows the voltammetric response for the same electrode in the same solution of $(Ru(v\text{-}tpy))_2(tppz)(PF_6)_4$ when the potential was scanned beyond the two-electron reduction at −1.50 V. The increase in current upon continuous scanning indicates that electropolymerization of the complex rapidly occurs (Figure 8B; note change in the current scale). Figure 8C depicts the voltammetric response observed when the electrode was scanned between 0.0 and −1.70 V for 5 min, rinsed with acetone, air-dried, and placed in a solution containing only supporting electrolyte. Well-defined and symmetric waves, typical of surface-confined redox centers, are observed at potentials that are virtually identical to those of the complex in solution.

In the positive potential region, similarly well-behaved redox responses are observed at potentials of +1.32 and +1.63 V. Again, these values are nearly identical to those of the complex in solution. Figure 7B shows a voltammogram in the positive region for an electrode modified at a coverage of 9.7×10^{-10} mol/cm^2 of the complex.

$Ru(tppz)_2(Ru(tppy))(PF_6)_4$. Since this complex is not symmetric, we would expect to observe the Ru centers to oxidize at different potentials even in the absence of any degree of interaction through the bridging ligand. In the positive potential region, this complex exhibits two oxidations at +1.38 and +1.68 V. The wave at +1.38 V is ascribed to the Ru center bound to a tppz and a tpy ligand. The process observed at +1.68 V is assigned to the Ru bound to a bridging and a peripheral tppz ligands since we would expect this oxidation to occur at a more positive potential. In the negative region, the complex undergoes two one-electron reductions at −0.39 and −0.85 V and a two-electron reduction at −1.43 V. We would expect the first wave to be a one-electron reduction of the peripheral ligands; however, we are not able to unequivocably assign the remaining processes.

$(Os(tpy))_2(tppz)(PF_6)_4$. This complex displays electrochemical behavior different from the analogous ruthenium dimetallic complex. The Os(II/III) oxidations are observed at +0.97 and +1.44 V (Figure 6B) and the difference in formal oxidation potentials ($\Delta E^{\circ\prime}$ = 470 mV) is larger than in the analogous ruthenium complex. This complex also displays a difference (110 mV) in formal potentials between its first oxidation and that in the monometallic mixed-ligand complex. The fact that in this case the $\Delta E^{\circ\prime}$ for the osmium complex is larger than that for the ruthenium analog would point to the importance of modulation in the π-back-bonding ability of the bridging pyrazine. However, such was not the case for the $[M_2(tppz)_3](PF_6)_4$ complexes. This would suggest that the pendant pyridines in these complexes are not innocent but rather may be playing a rather active role.

Similar to the analogous ruthenium complex, the dimetallic osmium complex exhibits two one-electron ligand-based reductions at −0.39 and −0.82 V corresponding to the first and second reductions of the bridging tppz ligand. These reductions are shifted positive relative to the corresponding processes in the monometallic mixed-ligand complex, indicating a significant degree of stabilization of the bridging tppz π^* orbitals. The two one-electron reductions at −1.35 and −1.45 V, which we attribute to the reduction of the peripheral terpyridine ligands, lead to adsorption of the complex on the electrode surface. When the potential is scanned beyond −1.45, there is a sharp desorption spike upon scan reversal at −1.32 V (Figure 5). As previously mentioned for the other dimetallic complexes, when the complex is reduced by four electrons, it is neutral and apparently less soluble in the acetonitrile solution and thus prone to precipitation on the electrode surface.

((tpy)Os(tppz)Ru(tpy))$(PF_6)_4$. This heterodimetallic complex displays two reversible, one-electron oxidations at +1.11 and +1.38 V (Figure 6C). Since for similar coordination, the Ru(II/III) oxidations take place at more positive potentials than the Os(II/III) couples, we attribute the first oxidation at +1.11 V to the Os(II/III) couple and that at +1.38 V to the Ru(II/III) couple. As in previous cases, the reductions of the bridging tppz ligand are observed as one-electron reductions at −0.41 and −0.85 V. The complex also exhibits a two-electron reduction at −1.55 V, which, as in the previous cases, we attribute to the simultaneous reduction of the peripheral terpyridine ligands. This complex, however, does not appear to precipitate when present as a neutral species.

$(Ru(tpy))_2Os(tppz)_2(PF_6)_6$. The voltammetric response of the heterotrimetallic species containing one central osmium and two peripheral ruthenium metal centers, $(Ru(tpy))_2Os(tppz)_2(PF_6)_6$, is shown in Figures 9 and 10. At positive potentials, this complex has three one-electron oxidations at +1.23, +1.59, and +1.72 V (Figure 9). We ascribe the first wave at +1.23 V to the Os(II/III) center since it is at the same potential as $Os(tppz)_2(PF_6)_2$, and as mentioned above, we would expect the osmium center to oxidize at a less positive potential than the ruthenium centers. We ascribe the two oxidation processes at +1.59 and +1.72 V to Ru(II/III) oxidations.

The oxidation potential for osmium in this trimeric species is virtually identical to that in $[Os(tppz)_2](PF_6)_2$, suggesting that

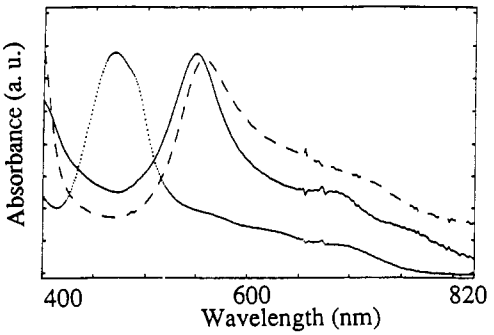

Figure 11. Visible spectra in acetonitrile solutions of (···) $Os(tpy)(tppz)^{+2}$ (2.00×10^{-5} M), (—) $(tpy)Os(tppz)Os(tpy)^{4+}$ (2.08×10^{-5} M), and (– –) $(tpy)Ru(tppz)Os(tppz)Ru(tpy)^{+6}$ (5.40×10^{-6} M).

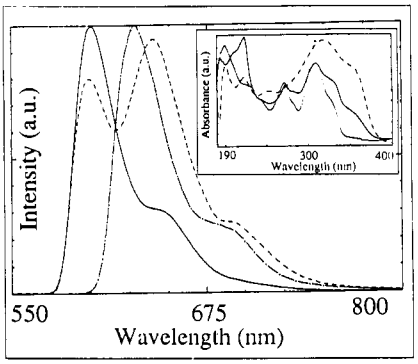

Figure 12. Luminescence spectra of (—) $Ru(tpy)_2^{2+}$ [1.87×10^{-5} M] (intensity × 1.17), (– · –) $Ru(tppz)_2^{2+}$ [4.30×10^{-5} M] (intensity × 1), and (– –) $Ru(tpy)(tppz)^{2+}$ [2.47×10^{-4} M] (intensity × 1.24) in ethanol/methanol (4:1) solutions at 77 K upon irradiation with λ = 470, 480, and 468 nm, respectively. Inset: absorption spectra.

the presence of the ruthenium centers has a very minor effect. Similarly the potential for the first oxidation of the ruthenium center (+1.59 V) is shifted by a relatively modest amount (relative to other values observed in this study) when compared to the value for $[Ru(tpy)(tppz)](PF_6)_2$ (+1.50 V).

However, the significant difference in oxidation potentials for the ruthenium centers ($\Delta E^{\circ\prime}$ = 130 mV) implies a significant degree of interaction. Given the large Ru–Ru distance in this complex (ca. 30 Å), it is quite remarkable to observe such a degree of interaction through the central $Os(tppz)_2$ unit. At negative potentials, the complex undergoes four reversible one-electron reductions that correspond to the sequential reductions of the tppz ligands. These appear as two sets of two waves indicating the reduction of each bridging tppz by one and two electrons, respectively.

This complex was also found to adsorb on the electrode surface. As shown in Figure 10, as the potential is scanned negatively and reversed at –1.10 V, the four processes at –0.30, –0.42, –0.82, and –0.97 V appear reversible and their respective peak current ratios are equal to 1. If the potential is scanned past –1.46 V, the potential at which the peripheral terpyridine ligands are reduced, upon scan reversal, a sharp desorption peak is observed at –1.33 V and a smaller one at –0.82 V.

In order to determine whether the complex remained on the electrode surface, the potential was scanned negatively to –1.50 V and held there for approximately 4 min after which the electrode was removed from solution, rinsed with acetone and transferred to a cell which contained aqueous 0.1 M $NaClO_4$ solution. When the potential was scanned in the positive direction, a surface wave corresponding to the Os(II/III) oxidation was observed (as shown in the inset to Figure 9) with a formal potential of +1.17 V and a peak separation of 120 mV. This wave was stable to scanning past this oxidation. In the negative direction, the first reductions of the bridging tppz ligands are observed as reversible one-electron waves at –0.47 and –0.63 V, as shown in the inset to Figure 10. The second reductions of the tppz bridging ligands are observed as one broad wave centered at –1.10 V. The adsorbed complex appeared to be stable on the surface when scanning negatively to –0.70 V. When the scan is reversed immediately after the first reduction of the tppz ligands, the peak current ratios of both waves were equal to 1. If the potential was scanned beyond the second set of reductions and reversed at –1.30 V, the peak current ratios of all the waves decreased and there was loss of material from the surface. The surface coverage of the complex on the electrode was determined to be 5.0×10^{-8} mol/cm^2 or approximately 80 monolayers. The large difference in potentials between the cathodic peak and the anodic peak was attributed to kinetic limitations in charge propagation through such a thick film of material.

Spectroscopic Measurements. Monomeric Complexes. Spectroscopic data for tppz and its complexes with ruthenium and osmium are compiled in Table III. The UV spectrum of the free tppz ligand showed four intense ($\epsilon = (0.8–1.6) \times 10^4$ (cm M)$^{-1}$) bands at 206, 224, 276, and 308 nm. In acidic solution (20% concentrated HPF_6 in acetonitrile), where all nitrogens are expected to be protonated and therefore mimic the electrostatic effect of coordination to a metal center, these bands were shifted to slightly lower energies (Table III). In $Ru(tppz)_2^{2+}$, these ligand-localized transitions were observed at 202, 254, 318, and 357 nm. The osmium complex, $Os(tppz)_2^{2+}$ exhibits a similar spectrum with absorptions at 204, 254, 326, and 350 nm. All four of these bands were observed in complexes with the general formula $M(tppz)_2(PF_6)_2$, where M = Fe, Ru, and Os, and, therefore, were assigned as π–π^* transitions.

The UV spectra of the mixed-ligand complexes $M(tpy)(tppz)^{2+}$ demonstrate that the ligand-centered (LC) transitions observed in the region between 190 and 400 nm are approximately additive. As shown in the inset to Figure 12, the absorption spectrum of $Ru(tpy)(tppz)^{2+}$ is approximately a composite of the spectra of $Ru(tppz)_2^{2+}$ and $Ru(tpy)_2^{2+}$ (all three spectra are shown for comparison purposes). In addition to the π–π^* transitions observed in $Ru(tppz)_2^{2+}$, the mixed-ligand complex $Ru(tpy)(tppz)^{2+}$ exhibits absorptions at 274 and 334 nm which are both characteristic of the spectrum of $Ru(tpy)_2^{2+}$. The UV spectrum of $Os(tpy)(tppz)^{2+}$ also exhibits the same additive behavior (Table III).

All monomeric complexes exhibit an absorption band between 470 and 478 nm which we ascribe to a d_{π}–π^* MLCT transition. $Ru(tppz)_2^{2+}$ and $Os(tppz)_2^{2+}$ have absorptions at 478 and 470 nm, respectively, which are at very similar energies to those observed in the corresponding terpyridine complexes (Table III). The mixed-ligand complexes $M(tpy)(tppz)^{2+}$ also exhibited an absorption band in the visible region at 476 and 470 nm for the ruthenium and osmium complexes, respectively.

Dimetallic and Trimetallic Complexes. The UV spectra of the dimetallic and trimetallic complexes were found to involve π–π^* transitions in both peripheral and bridging ligands. As would be anticipated, in the spectra of complexes in which tppz acts as a bridging ligand, these π–π^* transitions are shifted to lower energies given the stabilization of its π^*-accepting orbitals upon coordination to a second metal center. The MLCT transitions in dimetallic complexes were observed in the region 548–550 nm. These values also represent a significant shift to lower energies with respect to those observed in the monomeric complexes (470–478 nm). In the spectrum of the trimetallic complex studied, $Os(tppz)_2(Ru\text{-}tpy)_2^{6+}$, the MLCT transition was shifted to slightly lower energy at 556 nm. Figure 11 shows the visible absorption spectra of $Os(tpy)(tppz)^{2+}$, $(Os(tpy))_2tppz^{4+}$, and $Os(tppz)_2(Ru(tpy))_2^{6+}$ in acetonitrile solutions, which clearly demonstrates the progressive decrease in absorption energies.

Luminescence Properties. Monometallic Complexes. All monomeric complexes of Os and Ru with tppz were found to be luminescent at both ambient and low (liquid-nitrogen) temper-

Table III. Electronic Spectra of tppz and Its Complexes with Ru(II) and Os(II) and Related Materials at Room Temperature in Acetonitrile

complex	λ_{max} (nm)	ϵ (10^{-4} cm^{-1} M^{-1})	complex	λ_{max} (nm)	ϵ (10^{-4} cm^{-1} M^{-1})
		Free Ligands:			
tppz	206	0.80	tppz[d]	200	0.43
[4.74 × 10^{-5} M]	224	1.58	[9.00 × 10^{-5} M]	214	0.95
	276	1.57		278	0.80
	308	1.59		340	1.08
		Monomeric Complexes			
$Ru(tpy)_2(PF_6)_2$[a]	202	6.82		334	sh
[6.80 × 10^{-6} M]	232	sh		355	sh
	243	sh		476	0.308
	272	4.24	$Os(tpy)_2(PF_6)_2$[c]	210	4.85
	308	7.04	[1.02 × 10^{-5} M]	232	4.60
	335	sh		272	4.32
	476	1.58		312	4.83
$Ru(tppz)_2(PF_6)_2$[b]	200	14.6		478	1.10
[1.00 × 10^{-6} M]	222	12.5	$Os(tppz)_2(PF_6)_2$	204	4.85
	254	9.95	[1.26 × 10^{-5} M]	254	3.55
	318	19.3		326	6.52
	357	sh		350	sh
	478	6.23		470	2.01
$Ru(tpy)(tppz)(PF_6)_2$[b]	194	1.08	$Os(tpy)(tppz)(PF_6)_2$	206	4.18
[4.34 × 10^{-6} M]	224	1.33	[2.00 × 10^{-5} M]	274	2.90
	274	1.00		316	4.06
	283	sh		470	1.08
	310	1.06			
		Dimeric Complexes			
$Ru_2(tppz)_3(PF_6)_4$	202	8.89		306	3.88
[9.03 × 10^{-6} M]	256	3.25		362	2.11
	298	4.28		550	1.66
	325	sh	((tpy)Os)(tppz)(Ru(tpy))$(PF_6)_4$	198	1.21
	354	sh	[4.63 × 10^{-5} M]	243	sh
	550	1.94		274	0.750
$Os_2(tppz)_3(PF_6)_4$	204	7.87		283	sh
[1.02 × 10^{-5} M]	258	5.52		302	1.03
	300	sh		338	sh
	328	7.90		376	0.473
	554	3.00		400	sh
$((tpy)Ru)_2(tppz)(PF_6)_4$[b]	196	8.52		546	4.39
[9.15 × 10^{-6} M]	242	3.65	$Ru(tppz)_2(Ru(tpy))(PF_6)_4$	202	12.0
	274	4.99	[6.70 × 10^{-6} M]	244	sh
	300	6.94		274	6.99
	332	3.44		300	9.75
	374	3.30		322	4.77
	548	3.60		376	4.67
$((tpy)Os)_2(tppz)(PF_6)_4$	208	3.38		548	5.07
[2.08 × 10^{-5} M]	274	3.30			
		Trimetallic Complex			
$((tpy)Ru)_2Os(tppz)_2(PF_6)_6$	202	14.5		332	6.5
[5.40 × 10^{-6} M]	245	sh		376	6.85
	274	7.49		556	5.32
	300	1.12			

[a] Reference 12a. [b] Reference 9. [c] Reference 12c. [d] In 20% HPF_6.

Table IV. Luminescence Data for Monometallic Complexes of Ru(II) and Os(II) Polypyridyl Complexes in Ethanol/Methanol (4:1) in nm

complex	λ_{ex}[e]	concn (M)	$\lambda_{298\ K}$	$\lambda_{77\ K}$
$Ru(tpy)_2(PF_6)_2$[a]	478	2.71 × 10^{-5}		600 (644)[c]
$Ru(tppz)_2(PF_6)_2$[d]	480	4.31 × 10^{-5}	648	628 (691)
$Ru(tpy)(tppz)(PF_6)_2$	470	2.47 × 10^{-5}	670	600, 640 (691)
$Os(tpy)_2(PF_6)_2$[b]	470	1.56 × 10^{-5}	710	698 (798)
$Os(tppz)_2(PF_6)_2$	467	2.60 × 10^{-5}	731	740
$Os(tpy)(tppz)(PF_6)_2$	478	1.44 × 10^{-4}	770	643 (698), 746

[a] Reference 12a,b. [b] Reference 12c. [c] Shoulder given in parentheses. [d] Reference 9. [e] λ_{ex} refers to excitation wavelength.

atures. All luminescence data for Os and Ru monomeric complexes with tppz and related complexes are presented in Table IV. In an ethanol/methanol (4:1) solution, $Ru(tppz)_2^{2+}$ exhibits a room-temperature emission maximum at 648 nm whereas the corresponding terpyridine complex does not emit at room temperature.[12] At low temperature (77 K) this emission is more intense and blue-shifted to 628 nm with a shoulder at 691 nm (Figure 12). Both room- and low-temperature emissions are observed at lower energies relative to that observed in solutions of $Ru(tpy)_2^{2+}$,[12] (λ_{max} = 600 nm at 77 K), which is to be expected given the lower lying π^*-system in tppz relative to terpyridine. The monomeric osmium complex $Os(tppz)_2^{2+}$ has a room-temperature emission at 740 nm and a much more intense emission at 77 K at 731 nm (Figure 13). This emission is also red-shifted with respect to that observed in a solution of $Os(tpy)_2^{2+}$ (λ_{max} = 698 nm)[12c] (Figure 12).

At room temperature, the mixed-ligand complex $Ru(tpy)(tppz)^{2+}$ has a broad emission band at 670 nm. At 77 K, this band is resolved into two sharper and more intense emissions at 600 and 640 nm, respectively, with a shoulder at 691 nm (Figure 12). The excitation spectrum reveals that both emissions are generated by a broad absorption centered at 470 nm, which is to be expected, since both $Ru(tppz)_2^{2+}$ and $Ru(tpy)_2^{2+}$ have MLCT absorptions at that energy. In an attempt to better understand the nature of these emitting states, the spectra of all monomers were taken in highly acidic solution containing ethanol/methanol (4:1) and 20% concentrated HPF_6. In such an acidic medium, we would expect that protonation of all uncoordinated pyridines

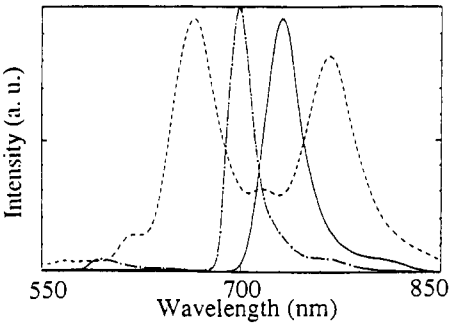

Figure 13. Luminescence spectra of (– • –) $Os(tpy)_2^{2+}$ [1.56×10^{-5} M] (intensity × 1), (—) $Os(tppz)_2^{2+}$ [2.60×10^{-5} M] (intensity × 2.82), and (- - -) $Os(tpy)(tppz)^{2+}$ [1.44×10^{-5} M] (intensity × 25.75) in ethanol/methanol (4:1) solutions at 77 K upon irradiation with λ = 478, 467, and 478 nm, respectively.

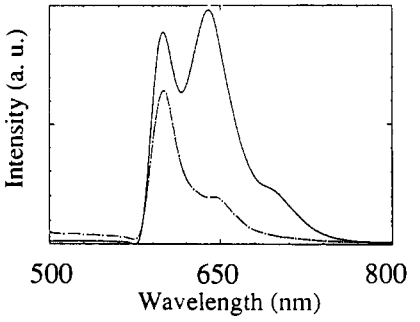

Figure 14. Luminescence spectra of $Ru(tpy)(tppz)^{2+}$ in ethanol/methanol (4:1) at 77 K with (– • –) and without (—) HPF_6. $[Ru(tpy)(tppz)^{2+}]$ = 2.70×10^{-5} and 2.47×10^{-5} M, respectively.

in tppz would give rise to a shift in the emission energy of $M(tppz)_2^{2+}$ and in the mixed-ligand complexes. As anticipated since there are no uncoordinated groups, the low-temperature luminescence spectrum of $Ru(tpy)_2^{2+}$ in the acidic medium remained unchanged, exhibiting an intense emission at 600 nm with a shoulder at 649 nm. In the same acidic medium, the luminescence spectrum of $Ru(tppz)_2^{2+}$ changed to a much weaker emission that was slightly red-shifted to 664 nm. As shown in Figure 14, the luminescence spectrum of the mixed-ligand complex $Ru(tpy)(tppz)^{2+}$ in the same acidic medium exhibited only one emission at 600 nm with a shoulder at 640 nm. Since this emission appeared to be unaffected by the acidity of the medium, it is probably due to a luminescent state mostly localized on the terpyridine ligand. The emission at 640 nm in the mixed-ligand complex is therefore ascribed to a tppz-localized excited state. The emission spectra of $Ru(tpy)(tppz)^{2+}$, $Ru(tpy)_2^{2+}$, and $Ru(tppz)_2^{2+}$ are shown in Figure 12 for comparison purposes.

The analogous osmium complex $Os(tpy)(tppz)(PF_6)_2$ exhibits a broad emission at 770 nm at room temperature. In frozen ethanol/methanol glass at 77 K, this broad band is resolved into two intense bands at 643 (with a shoulder at 698 nm) and 746 nm, respectively. The luminescence spectra for $Os(tppz)_2^{2+}$, $Os(tpy)_2^{2+}$, and the mixed-ligand complex $Os(tpy)(tppz)^{2+}$ are shown in Figure 13. No luminescence was observed in acidic solutions for either $Os(tppz)_2^{2+}$ or $Os(tpy)(tppz)^{2+}$.

Dimetallic Complexes. As would be anticipated for dimetallic complexes with a great degree of metal–metal interactions through the bridging ligands, the MLCT transitions do not generate any emitting states. These complexes show no emissions when irradiated with λ = 550–560 nm.

Conclusions. We have found Ru and Os tppz complexes to be luminescent at both room and liquid-nitrogen temperatures. In the case of binary mixed-ligand complexes, emissions arise from excited states localized at each ligand. In addition, tppz acts as a very effective bridging ligand in the synthesis of a variety of dimetallic and trimetallic complexes. The differences observed in the metal-based oxidation potentials between metal centers in the homodimetallic complexes suggest metal–metal interactions through the bridging tppz ligand. Given the ability of tppz to act as a strong bridging ligand between metal centers, we believe that it might be possible to prepare higher oligomers whose electronic structure might provide the onset of band formation and the preparation of molecular wires. These complexes might provide an entry into a family of materials with potentially useful and new electronic and/or electrocatalytic properties. We are currently exploring the preparation and characterization of such materials.

Acknowledgment. Dr. Anthony Alexander is gratefully acknowledged for performing all the mass spectral analyses presented in this paper. This work was supported by the Materials Science Center at Cornell University.

Supplementary Material Available: A table of FAB mass spectral data (4 pages). Ordering information is given on any current masthead page.